Supplement of The Cryosphere, 12, 1957–1968, 2018
https://doi.org/10.5194/tc-12-1957-2018-supplement

The Cryosphere Open Access EGU

Supplement of

Microtopographic control on the ground thermal regime in ice wedge polygons

Charles J. Abolt et al.

Correspondence to: Charles J. Abolt (chuck.abolt@beg.utexas.edu)

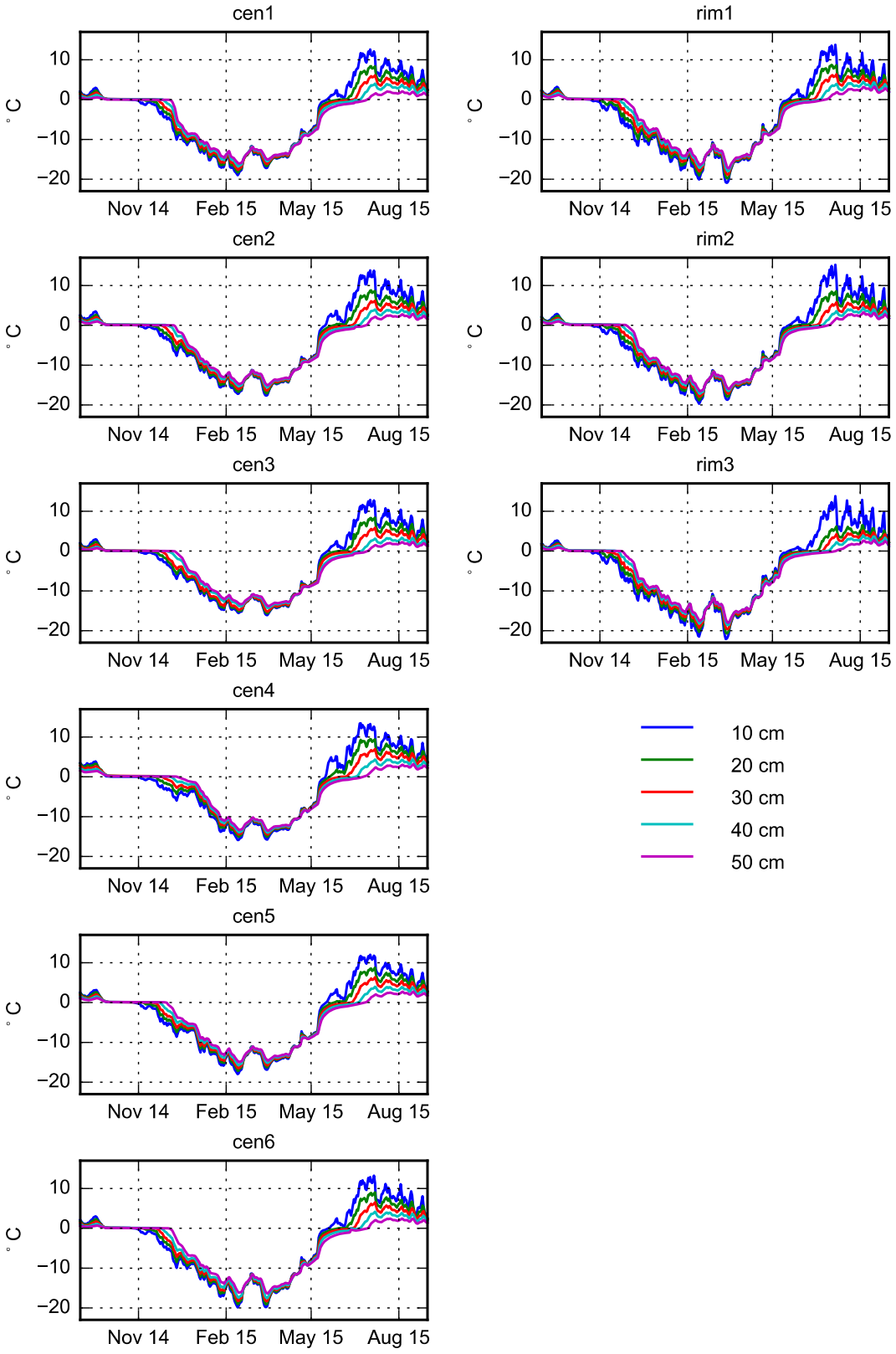

Figure S1. Observed temperature at each sensor rod

Text S1. Description of model calibration

In the first iteration of model construction and calibration, we conducted simulations using a one-dimensional domain, to speed up computational times while coarse tuning the model. The 1D domain preserved the same layering as the 2D mesh but did not include ice wedge cells. The domain was 50 m deep, and the same boundary conditions were applied as in the 2D simulations.

The sole parameter tuned during 1D simulations was a snowfall multiplication factor. It is well-known that records of snowfall frequently underestimate the real precipitation rate. A study of 10 National Weather Service stations in Alaska, for example, found snowfall estimates were systematically underestimated by as much as 140% (Yang et al., 1998), and Atchley et al. (2015) found it necessary to augment snowfall rates observed at a weather station near Barrow, AK ~40% to reproduce the active layer thermal regime in 1D thermal hydrology simulations. Our meteorological data was sourced from the output of the Noah Land Surface Model associated with NASA's Global Land Data Assimilation System (GLDAS), which is influenced by local ground-based measurements (Rodell et al., 2004).To compensate for potential underestimation of snowfall in our meteorological data, we ran a set of simulations in which GLDAS snowfall was increased by factors of 0-100% in increments of 10%. Following each simulation, we extracted temperatures at depths of 10, 20, 30, 40, and 50 cm for comparison with observational data from rod cen1, which was intermediate in elevation among the sensor rods. The best performing multiplication factor was 1.8, which we interpreted as providing a rough estimate of the true snowfall rate.

In the second stage of model calibration we expanded into 2D simulations. During this stage, two additional snowpack parameters were tuned heuristically. The first, snow thermal conductivity, is represented in the Advanced Terrestrial Simulator (ATS) (Atchley et al., 2015; Painter et al., 2016) as an empirical function of snow density (which increases with age) (Goodrich, 1982). By default, ATS assigns fresh snow a density of 100 kg m^{-3} and a thermal conductivity of 0.029 W m^{-1} K^{-1}. We explored values between half and double the default thermal conductivity, in accordance with recent measurements by Domine et al. (2016) and Riche and Scheebeli (2013). The second parameter we tuned was the diffusion-like coefficient used by ATS to redistribute snow across topography. We explored values within an order of magnitude in either direction of its default, effectively altering the speed with which the snowpack develops a level surface during the course of winter. In addition to these two parameters, we explored values of the snowfall augmentation factor within ±20% of the coarse-tuned estimate from the 1D simulations. Following every 2D run, we extracted simulated temperature from 2014-2015 for comparison with observations at the five rods intersecting the transect, then made a decision in which direction to tune each parameter.

Text S2. Estimation of soil physical parameters from core samples

The water retention curve in ATS is parameterized using the Van Genuchten model. Necessary parameters include saturated volumetric water content (θ_s, $m^3\ m^{-3}$), residual water content (θ_r, $m^3\ m^{-3}$), inverse air entry potential (α, cm^{-1}), and the shape parameter, m (unitless). We estimated the Van Genuchten parameters for each soil core using a HYPROP system (METER Group, Pullman, Washington, USA), which employs the Wind evaporation method (Wind, 1968) to estimate unsaturated hydraulic properties while an initially saturated soil sample is left to dry. Soil cores had been collected in steel rings, five centimeters tall and eight centimeters in diameter. The HYPROP system includes two tensiometers, inserted at depths of 1.25cm and 3.75cm, which record water potential as the core is allowed to evaporate through its top face. The mass flux of water leaving the core is monitored by conducting the experiment on top of a balance. After the tensiometers cavitate, software provided by the manufacturer fits an inverse model based on the Richards Equation to the time series data of tension and evaporative flux. To provide additional data points for the parameter estimation algorithm, we also estimated soil water potential in air-dry subsamples from each core using a WP4 Dewpoint Potentiometer (METER Group), which infers soil water potential by measuring the relative humidity of air in equilibrium with a sample.

Soil thermal properties used as input by ATS include thermal conductivity of saturated, thawed soil (λ_s, $W\ m^{-1}\ K^{-1}$), and thermal conductivity of dry soil material (λ_u, $W\ m^{-1}\ K^{-1}$). The thermal conductivity of soil at intermediate states of liquid or ice saturation is derived from these values and from the water retention curve, using equations described in Atchley et al. (2015). We estimated soil thermal conductivity using a KD2 Pro dual-needle heat pulse probe (METER Group), which was inserted into the top of the soil core during the evaporation experiments described in the previous paragraph. The KD2 estimates soil thermal properties at a depth of 1.25 cm below the surface, the same depth as the upper tensiometer of the HYPROP. We programmed the KD2 to estimate thermal properties every thirty minutes while the core evaporated, and used the record of tension from the upper tensiometer to match the time series of thermal conductivity estimates with volumetric wetness values. Following cavitation, we extrapolated these data points to 0% volumetric water content, to estimate the thermal conductivity of dry soil material.

Hydraulic and thermal properties from each core, estimated through these procedures, are presented in Table S1.

Table S1. Estimated soil hydraulic and thermal properties from field samples

Location	Depth *cm*	Saturated water content θ_s $m^3\ m^{-3}$	Residual water content θ_r $m^3\ m^{-3}$	Van Genuchten parameter α cm^{-1}	Van Genuchten parameter m *unitless*	Saturated (thawed) thermal conductivity λ_s $W\ m^{-1}\ K^{-1}$	Dry thermal conductivity λ_u $W\ m^{-1}\ K^{-1}$	Ground material
Center	0	0.75	0.08	0.02	0.41	0.68	0.1	Upper peat
Center	12	0.62	0.06	0.02	0.49	1.34	0.2	Lower peat
Rim	0	0.74	0.00	0.04	0.26	0.68	0.12	Upper peat
Rim	8	0.68	0.02	0.02	0.33	0.84	0.15	Lower peat
Rim	19	0.76	0.03	0.02	0.32	0.79	0.15	Lower peat
Rim-Center boundary	0	0.66	0.00	0.09	0.32	0.52	0.15	Upper peat
Rim-Center boundary	12	0.65	0.04	0.02	0.41	0.64	0.12	Lower peat
Rim-Center boundary	19	0.66	0.07	0.02	0.46	0.94	0.2	Lower peat

References

Atchley, A. L., Painter, S. L., Harp, D. R., Coon, E. T., Wilson, C. J., Liljedahl, A. K. and Romanovsky, V. E.: Using field observations to inform thermal hydrology models of permafrost dynamics with ATS (v0.83), Geoscientific Model Development, 8(9), 2701–2722, doi:10.5194/gmd-8-2701-2015, 2015.

Domine, F., Barrere, M. and Sarrazin, D.: Seasonal evolution of the effective thermal conductivity of the snow and the soil in high Arctic herb tundra at Bylot Island, Canada, The Cryosphere, 10(6), 2573–2588, doi:10.5194/tc-10-2573-2016, 2016.

Goodrich, L. E.: The influence of snow cover on the ground thermal regime, Canadian geotechnical journal, 19(4), 421–432, 1982.

Painter, S. L., Coon, E. T., Atchley, A. L., Berndt, M., Garimella, R., Moulton, J. D., Svyatskiy, D. and Wilson, C. J.: Integrated surface/subsurface permafrost thermal hydrology: Model formulation and proof-of-concept simulations, Water Resources Research, doi:10.1002/2015WR018427, 2016.

Riche, F. and Schneebeli, M.: Thermal conductivity of snow measured by three independent methods and anisotropy considerations, The Cryosphere, 7(1), 217–227, doi:10.5194/tc-7-217-2013, 2013.

Rodell, M., Houser, P. R., Jambor, U., Gottschalck, J., Mitchell, K., Meng, C.-J., Arsenault, K., Cosgrove, B., Radakovich, J., Bosilovich, M., Entin, J. K., Walker, J. P., Lohmann, D. and Toll, D.: The Global Land Data Assimilation System, Bulletin of the American Meteorological Society, 85(3), 381–394, doi:10.1175/BAMS-85-3-381, 2004.

Wind, G. P.: Capillary conductivity data estimated by a simple method, in Water in the unsaturated zone: Proceedings of the Wageningen Symposium, vol. 1, pp. 181–191, International Association of Scientific Hydrology, 1969.

Yang, D., Goodison, B. E., Ishida, S. and Benson, C. S.: Adjustment of daily precipitation data at 10 climate stations in Alaska: Application of World Meteorological Organization intercomparison results, Water Resources Research, 34(2), 241–256, 1998.